tvst

https://doi.org/10.1167/tvst.8.1.2

Article

Characterization of Corneal Epithelial Cells in Keratoconus

Rohit Shetty[1], Krishna Poojita Vunnava[1], Kamesh Dhamodaran[2,3], Himanshu Matalia[1], Subramani Murali[2], Chaitra Jayadev[4], Ponnulagu Murugeswari[2], Arkasubhra Ghosh[5], and Debashish Das[2]

[1] Department of Cornea and Refractive Surgery, Narayana Nethralaya Eye Institute, Bangalore, Karnataka, India
[2] Stem Cell Research Laboratory, GROW Laboratory, Narayana Nethralaya Foundation, Bangalore, Karnataka, India
[3] Current address: Department of Basic Sciences, The Ocular Surface Institute, College of Optometry, University of Houston, Houston, TX, USA
[4] Department of Vitreo-Retinal Services, Narayana Nethralaya Eye Institute, Bangalore, Karnataka, India
[5] GROW Laboratory, Narayana Nethralaya Foundation, Bangalore, Karnataka, India

Correspondence: Debashish Das, Stem Cell Research Laboratory, GROW Laboratory, Narayana Nethralaya Foundation, Narayana Nethralaya Eye Hospital, Narayana Health, Bommasandra, Bangalore-560 099, Karnataka, India. e-mail: dasdebashish@yahoo.co.uk; drdebashish@narayananethralaya.com

Received: 1 May 2018
Accepted: 9 November 2018
Published: 3 January 2019

Keywords: corneal epithelial cells; keratoconus; corneal crosslinking; apoptosis; proliferation; epithelial-mesenchymal transition

Citation: Shetty R, Vunnava KP, Dhamodaran K, Matalia H, Murali S, Jayadev C, Murugeswari P, Ghosh A, Das D. Characterization of corneal epithelial cells in keratoconus. Trans Vis Sci Tech. 2019;8(1):2, https://doi.org/10.1167/tvst.8.1.2

Purpose: We studied the cellular characteristics of epithelial cells in the cone and extraconal periphery of corneas in keratoconus eyes.

Methods: This prospective observational study was conducted at Narayana Nethralaya Eye Institute. A total of 83 and 42 eyes with keratoconus and normal topography, respectively, were included in the study. Corneal epithelial cells were collected and analyzed for apoptosis, proliferation, epithelial-mesenchymal transition, and differentiation status using molecular and biochemical tools. Statistical analysis was performed using the Student's *t*-test.

Results: Corneal epithelial cells from the cone showed significantly higher expression of proapoptotic marker BAX ($P < 0.005$) compared to controls. Significantly elevated expression of cell cycle markers CYCLIN D1 ($P < 0.005$) and Ki67 ($P < 0.005$) were noted in the extraconal region compared to controls. Cells of the cone showed significantly higher ZO-1 ($P < 0.005$) and lower vimentin ($P < 0.005$) compared to controls. Significantly lower expression of the differentiation marker CK3/12 ($P < 0.05$) was observed in cones compared to controls.

Conclusions: Cones of keratoconic corneas show enhanced cell death, poor differentiation, proliferation and epithelial-mesenchymal transition. The cellular changes of the corneal epithelial cells in the cone and extraconal region differ significantly in a keratoconus corneas.

Translational Relevance: Characterization of patient-specific corneal epithelial cellular status in keratoconus has the potential to determine the optimal treatment and therapeutic outcomes paving the way towards personalized treatment in the future.

Introduction

Keratoconus (KC) is a corneal ectatic disease resulting from progressive focal thinning of the cornea causing irregular astigmatism and blurring of vision.[1,2] Disease progression is observed to be variable, with the involvement of multiple genes as well as environmental factors.[3] Though the exact etiology of KC remains elusive, inflammation is a key factor that influences the severity of the disease. We previously have shown elevated levels of matrix metalloprotease 9 (MMP9) and interleukin-6 (IL-6) with a concurrent reduction in lysyl oxidase, collagen1A1, and collagen IVA1 with increasing severity of the disease.[4,5]

Though KC is thought to involve the entire cornea, a topographically distinct pattern remains with the maximum deformity seen over the apex of the cone with a surrounding unaffected periphery.[6] This localized distinction of the KC cornea into cone and extraconal periphery zones underpins a differential cellular signature. Though apoptosis of keratocytes is a hallmark of KC corneas, the altered

turnover of corneal epithelial cells might contribute to the thinning of the cornea as well. Morphologic studies have revealed higher numbers of normal epithelial cells in the keratoconic periphery whereas the cells in the apex of cone were elongated and arranged in whorl-like fashion.[7] A primary pathologic issue in the KC cornea has been thought to be the disease associated apoptosis in the stroma and possibly the epithelium, leading to a thinning of these corneal layers.[8] Studies using wound healing assays have revealed that an apoptotic corneal epithelium can lead to death of keratoycytes.[9,10] Moreover, higher number of apoptotic cells were detected in the deeper levels in KC cornea compared to those that were only superficial in normal corneas.[8] Defective Bowman's membrane, dying keratocytes and thickening nerve fibers are the salient morphologic features of KC.[11]

Though corneal collagen crosslinking (CXL) for KC is a widely performed procedure, it still is not suitable for every patient.[12] The adverse effects of ultraviolet-A (UV-A) irradiation on the limbal epithelial stem cells residing in the proximity of the exposed cornea has been described by several groups.[13–15] Additionally, one feared complication of KC treatment with CXL is infectious keratitis secondary to nonhealing epithelium.[16,17] A better understanding of the role of corneal epithelial cells in KC may help determine the optimal treatment regime of CXL to ensure a safer treatment outcome.

Most studies are targeted towards understanding the consequences of the CXL procedure with respect to the biomechanical properties and tissue reorganization.[18–20] It is well established that the nature of corneal epithelial cells in the cone and extraconal periphery area of the cornea bear the plausible footprints of the treatment outcome. Shetty et al.[21] showed that corneal epithelial cells from KC cone with a higher expression LOX and lower expression of MMP9 are associated with better corneal flattening post crosslinking, whereas a reduced gene expression of COL IVA 1, BMP 7, and TIMP 1 correlated with suboptimal response to crosslinking.[21] There is a lack of knowledge about the expression status and signaling pathways of corneal epithelial cells in the ectatic cone area in KC patients. Hence, we studied the inherent characteristics of corneal epithelial cells in the cone as well as the extraconal periphery regions. These findings may provide insight in two aspects of KC, namely the association of gene expression of the ectatic zone specific corneal epithelial cells with the stromal thinning and disease severity. A possible clinical application of such data could be in identifying the high risk patient population that might be predisposed to suffer post-CXL corneal epithelial defects. Cellular and biochemical assays were performed to investigate the status of differentiation, apoptosis, proliferation, and epithelial-mesenchymal transition of corneal epithelial cells in KC eyes compared to controls.

Methods

Clinical Sample Details

This study was approved by the Narayana Nethralaya institutional review board and Narayana Nethralaya ethics committee (Bangalore, India) and adhered to the tenets of the Declaration of Helsinki. Informed written consent was obtained from all subjects. A total of 83 eyes with KC (31 grade I, 27 grade II and 25 grade III) and 42 with normal topography as controls (photorefractive keratectomy [PRK] group) were included in the study. No two eyes of a single patient were included in the KC or PRK group. Hence, a total of 125 biological samples were used in the study, including the KC and PRK groups.

KC was diagnosed based on the presence of one or more of the following signs: stromal thinning, focal protrusion or increase in corneal curvature, Fleischer's ring, Vogt's striae on slit-lamp examination, scissoring of the red reflex on retinoscopy, and curvature asymmetry leading to irregular corneal astigmatism and corneal elevation with corresponding thinning and steepening seen on Scheimpflug imaging. Eyes with progressive KC that needed CXL were divided into three groups based on the mean keratometry value that was obtained from the Pentacam Scheimpflug system (Oculus Optikgerate Gmbh, Germany). Grading was as follows: Grade I, $K_{mean} < 48$ D; Grade II, $K_{mean} < 52$ D; Grade III, $K_{mean} \geq 52$ D. Eyes of patients scheduled for PRK with a refractive error <5 diopters (D) and adequate corneal pachymetry for the procedure were screened thoroughly to rule out KC and considered as controls.

Collection of Corneal Epithelial Cells

After instillation of a topical anesthetic agent (proparacaine hydrochloride 0.5% solution, Akorn, Inc., Buffalo Groove, IL) and confirmation of the cone location from corneal topography maps, the epithelium was collected separately from the cone

region and the periphery using a manual scraper. During PRK, the epithelium from the corneal center and periphery was collected similarly. Corneal epithelial cells were collected in McCarey-Kaufman (MK; LV Prasad Eye Institute, Hyderabad, India) medium and stored at 4°C.

Real-Time Quantitative Polymerase Chain Reaction (RT-qPCR)

Total RNA was extracted from epithelial cells of KC and PRK samples using TRIzol reagent (Ambion, Carlsbad, CA). The extracted RNA was quantified using Nano Drop 1000 spectrophotometer (Thermo Fisher Scientific, Waltham, MA). Purity of the RNA was estimated by measure of absorption at 260/280 nm ratio within 1.8–2.0. Additionally, the integrity of the RNA was assessed using 1% agarose gel and detection of 28S and 18S rRNA bands wherein the intensity of the 28S band was approximately double of that of the 18S rRNA band. Based on the purity, 1000 ng RNA was converted to cDNA using the High-Capacity cDNA Reverse Transcriptase Kit (Life Technologies, Carlsbad, CA) according to the manufacturer's instructions and stored at −20°C. The cDNA used for RT-qPCR for differentiation, epithelial mesenchymal transition and notch signaling genes as described previously using the KAPPA SYBER FAST qPCR Master Mix (Kapa Biosystems, Wilmington, MA; Table 1).[13,22]

Trypan Blue Vital Staining

Viability of the corneal epithelial cells obtained intraoperatively was determined by staining with the supravital stain, trypan blue.[13] The number of viable cells and dead cells were counted. The percentages of viable cells are represented graphically in the Supplementary Figure. The trypan blue staining was observed under an Olympus CKX41phase contrast microscope (Olympus, Shinjuku, Tokyo, Japan), and images captured using the Olympus SP350.

Cytospin Smear Preparation

Corneal epithelial cells collected from eyes undergoing CXL and PRK in microcentrifuge tubes were pelleted and dissociated with Dispase II (2 mg/mL; Sigma-Aldrich Corp., St. Louis, MO). Cells were taken for a single cell layer smear using the Cytospin cytocentrifuge system (Thermo Shandon, Pittsburg, PA) on glass slides by centrifuging at 12*g* for 5 minutes. They were air dried and fixed with 4% cold paraformaldehyde (Sigma-Aldrich Corp.) for 10 minutes and washed once with PBS.

Immunostaining

Cytospin smeared corneal epithelial cells from KC and PRK were immunostained for different molecular markers. After fixing and washing, cells were permeabilized with 0.1% Triton X-100 (Fisher Scientific, Qualigens, Mumbai, India) and stained using antibodies as previously mentioned.[16] Stained cells were mounted using a VECTASHIELD containing 2-(4-amidinophenyl)-1H-indole-6-carboxamidine (Vector Laboratories, Burlingame, CA). Fluorescence images were captured using an Olympus BX41 fluorescent microscope with the Q.Capture Pro.7 software (Olympus; Table 2).

Western Blot

Samples for each grade of KC (Grade I, six; Grade II, five; Grade III, five biological samples) and PRK (five biological samples) were pooled and Western blot analysis was performed. Cells were lysed using the radioimmunoprecipitation assay (RIPA) buffer (G-Bioscience, St. Louis, MO). The total protein concentration was estimated using the BCA (Bicinchoninic acid) assay (Thermo Fisher Scientific). For Western blot analysis 20 µg protein was resolved on polyacrylamide gel electrophoresis. Three independent Western blots were analyzed using the same number of biological samples per grade of KC and PRK. In total, the number of biological samples used for Western blot analysis were KC 48 (Grade I, 18; Grade II, 15; Grade III, 15 biological samples) and PRK 15 biological samples. Protein bands were developed using an enhanced chemiluminescence detection kit (Pierce ECL Plus; Thermo Fisher Scientific) and analyzed with the Image Quant LAS 500 chemiluminescence detector (GE Healthcare Life Science, Uppsala, Sweden; Table 2).

Statistical Analysis

All experiments were performed at least in triplicate and results of independent experiments were used for statistical analysis. Data were represented as mean ± SD and were analyzed with Student's *t*-test calculated between control (PRK) and affected (KC) samples, cone and periphery, respectively. Significance values were $*P < 0.05$, $**P < 0.01$, $***P < 0.005$. The number of samples used for calculating the mean ± SD is stated in each of the Figure legends. *P* values along with the mean ± SD are shown in Table

Table 1. Primers Used in RT-qPCR

Serial No	Primer Name (RT-qPCR)	Sequences 5′-3′	Size, bp	Gene Accession No
1	*gapdh*	FP: ACCCACTCCTCCACCTTTGAC RP: TGTTGCTGTAGCCAAATTCGTT	100	NM_001289746.1
2	*bax*	FP: TTGCTTCAGGGTTTCATCCA RP: AGACACTCGCTCAGCTTCTTG	113	NM_138761
3	*bcl2*	FP: TGGCCAGGGTCAGAGTTAAA RP: TGGCCTCTCTTGCGGAGTA	143	NM_000633
4	*cyclin d1*	FP: AGCTCCTGTGCTGCGAAGTGGAAAC RP: AGTGTTCAATGAAATCGTGCGGGGT	133	NM_053056
5	*pcna*	FP: GCCAGAGCTCTTCCCTTACG RP: TAGCTGGTTTCGGCTTCAGG	87	NM_002592
6	*ki67*	FP: CTTTGGGTGCGACTTGACG RP: GTCGACCCCGCTCCTTTT	199	NM_002417
7	*cdc20*	FP: GTTCGGGTAGCAGAACACCA RP: CCCCTTGATGCTGGGTGAAT	187	NM_001255
8	*e-cadherin*	FP: AAGGAGGCGGAGAAGAGGAC RP: CGTCGTTACGAGTCACTTCAGG	87	NM_004360.3
9	*α-sma*	FP: GCTGGCATCCATGAAACCAC RP: TACATAGTGGTGCCCCCTGA	104	NM_001613.2
10	*fibronectin*	FP: TGGCCAGTCCTACAACCAGTA RP: CTCGGGAATCTTCTCTGTCAGC	119	NM_001306129.1
11	*ck3*	FP: AGTTTGCCTCCTTCATTGACA RP: TGCCTGAGATGGAACTTGTG	108	NM_057088.2
12	*ck12*	FP: ACGAGCTGACCCTGACCA RP: CGGAAGCTTTGGAGCTCAT	106	NM_000223.3
13	*notch 1*	FP: ATCCAGAGGCAAACGGAG RP: CACATGGCAACATCTAACCC	106	NM_017617
14	*notch 2*	FP: GGACCCTGTCATACCCTCTT RP: CATGCTTACGCTTTCGTTTT	150	NM_024408.3
15	*notch 3*	FP: GTGTGTGTCAATGGCTGGAC RP: GTGACACAGGAGGCCAGTCT	150	NM_000435.2
16	*notch 4*	FP: GAGGACAGCATTGGTCTCAAGG RP: CAACTCCATCCTCATCAACTTCTG	61	NM_004557.3
17	*dll1*	FP: GGCTACTCCGGCTTCAACT RP: ATCACCGAGGTCCACACACT	90	NM_005618.3
18	*dll3*	FP: AGCTCGTCCGTAGATTGGAA RP: AGCGTAGATGGAAGGAGCAG	81	NM_016941.3
19	*dll4*	FP: AAGGCTGCGCTACTCTTACC RP: AAGTGGTCATTGCGCTTCTT	90	NM_019074.3
20	*jagged 1*	FP: AAGGCTTCACGGGAACATAC RP: AGCCGTCACTACAGATGCAC	120	NM_000214
21	*jagged 2*	FP: GTCGTACTTGCACTCACAATACC RP: GTAGCAAGGCAGAGGGTTGC	51	NM_145159.2
22	*hes 3*	FP: GAAAGTCTCCCTGGCTCGTC RP: CCAAATAGGGAGCGCCTTCA	146	NM_001024598

Table 2. List of Primary and Secondary Antibodies

No	Name of Antibody	Dilution	Company
1	BAX, Mouse	1:250 (IF) 1:1000 (WB)	Abgenex, Bhubaneswar, India
2	BCL2 Rabbit	1:250 (IF)	Abgenex, Bhubaneswar, India
3	Ki67	1:250 (IF)	Abgenex, Bhubaneswar, India
4	CYCLIN D1, Mouse	1:1000 (WB)	Abgenex, Bhubaneswar, India
5	GAPDH, Mouse	1:1000 (WB)	Abgenex, Bhubaneswar, India
6	VIMENTIN, Rabbit	1:1000 (WB)	Abgenex, Bhubaneswar, India
7	ZO-1, Rabbit	1:100 (IF)	Boster Biologicals, CA
8	CK3/12, Mouse	1:60 (IF)	Abcam, Cambridge
9	JAGGED 2, Rabbit	1:1000 (WB)	Cell signaling, MA
10	NOTCH 1, Rabbit	1:1000 (WB)	Cell signaling, MA
11	Donkey anti-Rabbit IgG, Cy3	1:400 (IF)	Biolegend, CA
12	Goat anti-mouse IgG, Alexa Flour 488	1:250 (IF)	Abgenex, Bhubaneswar, India
13	Donkey anti-Rabbit IgG, HRP	1:4000 (WB)	Biolegend, CA
14	Goat anti-mouse IgG, HRP	1:4000 (WB)	Biolegend, CA

IF, Immunofluorescence; WB, Western blot.

3 (mRNA expression), Table 4 (densitometry analysis), and Table 5 (immunofluorescence quantification).

Results

Cellular Apoptosis Levels in the Cone and Extraconal Zones of KC Eyes

Corneal epithelial cells collected from controls as well as KC corneas were initially evaluated for cell viability using trypan blue staining. The results showed that approximately 80% to 90% of cells were viable before the experiments performed in the study (Supplementary Fig. S1). The ratio of the mRNA levels of *bax* and *bcl2* from corneal epithelial samples revealed higher expressions in the cone and periphery of KC eyes compared to the controls though the ratio was much higher for the cone area (Fig. 1A). Furthermore, Western blot revealed higher levels of BAX in cells obtained from the KC cone epithelium compared to the periphery. Densitometric analysis of the Western blot revealed a significant increase in the levels of BAX expression in the cones compared to the periphery (Figs. 1Bi–Bii). Immunofluorescence staining with BAX showed significantly increased positivity in the epithelial cells from cones and periphery with increasing grades of the disease compared to the controls (Fig. 1C). The percentage of increased positivity was much higher in the epithelial cells from cones compared to the periphery (Fig. 1E). Immunofluorescence staining of BCL2 showed a significant decrease in the number of positive cells in the cones and periphery of KC cornea epithelium compared to the controls. Additionally, the decrease was more significant ($P < 0.05$) in the diseased cones compared to the periphery (Figs. 1D, 1F).

Cellular Proliferation Status of the Cone and Extraconal Zone of KC Eyes

Expression of *cyclin D1, pcna, ki67*, and *cdc20* mRNA was analyzed to investigate the proliferative status of the corneal epithelial cells obtained from the affected cones and unaffected periphery compared to the controls. The results revealed significantly elevated levels of mRNA of the proliferative markers (*cyclin D1, pcna* and *ki67*) in the unaffected periphery compared to the controls. Moreover, the mRNA levels of *cyclin D1, pcna*, and *ki67* increased with increasing grades of disease severity (Fig. 2A). Gene expression studies were corroborated with CYCLIN D1 protein expression studies by Western blot (Fig. 2Di). Densitometric analysis of Western blot showed there was a significant up regulation in the levels of CYCLIN D1 protein levels in the extraconal periphery with increasing grades of KC (Fig. 2Dii). Immunofluorescence staining revealed significantly higher number of cells positive for Ki67 in the cells of the extraconal periphery compared to controls (Fig.

Table 3. Relative Fold Values of the mRNA Levels of Genes Obtained From RT-qPCR With *P* Values

	PRK		KC Grade I			
Gene	Ce[a]	P[b]	C[c]	*P* Value	*P*	*P* Value
bax:bcl2	1 ± 0.64	1 ± 0.44	1.9 ± 0.5	NS[d]	1.1 ± 0.4	NS
cyclin D1	1 ± 0.86	1 ± 0.86	2.7 ± 1.18	NS	3.2 ± 0.95	<0.05
pcna	1 ± 0.28	1 ± 0.16	1.18 ± 0.49	NS	2.12 ± 0.30	<0.005
ki67	1 ± 0.18	1 ± 0.43	1.35 ± 0.47	NS	3.01 ± 0.19	<0.005
cdc 20	1 ± 0.16	1 ± 0.51	0.94 ± 1.2	NS	2 ± 0.23	NS
alpha-SMA	6.7 ± 0.05	4.2 ± 0.02	6.7 ± 0.1	NS	7.2 ± 0.06	NS
fibronectin	9.3 ± 0.1	6.9 ± 0.4	9.6 ± 0.1	NS	11.2 ± 0.2	NS
ck3	1 ± 0.18	1 ± 0.21	0.72 ± 0.1	NS	1.23 ± 0.1	<0.05
ck12	1 ± 0.06	1 ± 0.04	0.73 ± 0.2	NS	1.39 ± 0.1	<0.01
notch 1	1 ± 0.2	1 ± 0.1	2.01 ± 0.4	<0.05	1.33 ± 0.3	NS
jagged 2	1 ± 0.09	1 ± 0.2	1.39 ± 0.01	<0.005	2.15 ± 0.004	<0.005
hes 3	1 ± 0.1	1 ± 0.27	1.47 ± 0.56	NS	2.16 ± 0.65	<0.01

[a] Center.
[b] Periphery.
[c] Cone.
[d] Nonsignificant.

Table 3. Extended

	KC Grade II				KC Grade III			
Gene	C	*P* Value	*P*	*P* Value	C	*P* Value	*P*	*P* Value
bax:bcl2	3.4 ± 0.6	<0.01	1.5 ± 0.7	NS	2.5 ± 0.5	<0.05	1.7 ± 0.6	NS
cyclin D1	2.26 ± 1.06	NS	10.5 ± 1.26	<0.005	5.8 ± 1.51	<0.01	13.1 ± 1.83	<0.005
pcna	1.13 ± 1.24	NS	3.13 ± 0.23	<0.005	1.16 ± 0.37	NS	7.11 ± 0.62	<0.005
ki67	1.94 ± 0.33	NS	4.02 ± 0.29	<0.005	2.72 ± 0.52	<0.01	6.03 ± 0.62	<0.005
cdc 20	1.31 ± 0.58	NS	2.75 ± 0.34	<0.01	1.23 ± 0.72	NS	3 ± 1.28	NS
alpha-SMA	7.0 ± 0.2	<0.01	7.4 ± 0.09	<0.005	6.8 ± 0.05	NS	8.2 ± 0.05	<0.005
fibronectin	9.2 ± 0.1	<0.005	10.6 ± 0.3	<0.005	9.07 ± 0.04	NS	9.4 ± 0.07	<0.005
ck3	0.58 ± 0.1	<0.05	1.43 ± 0.2	<0.01	0.35 ± 0.2	<0.05	1.21 ± 0.1	NS
ck12	0.52 ± 0.1	<0.05	1.41 ± 0.09	<0.01	0.40 ± 0.07	<0.01	0.88 ± 0.14	NS
notch 1	2.56 ± 0.3	<0.05	3.46 ± 0.	<0.005	3.42 ± 0.2	<0.005	4.93 ± 0.2	<0.005
jagged 2	1.43 ± 0.03	<0.005	2.39 ± 0.08	<0.005	1.44 ± 0.003	<0.005	2.46 ± 0.1	<0.005
hes 3	1.59 ± 0.75	<0.05	3.87 ± 0.069	<0.005	3.32 ± 0.07	<0.005	10.51 ± 0.65	<0.005

2B). Quantification showed a significantly higher percentage of Ki67-positive population in the extraconal periphery compared to control levels across all grades of KC (Fig. 2C).

Epithelial-Mesenchymal Transition in the Cone and Extraconal Zones of KC Eyes

Quantitative reverse transcriptase polymerase chain reaction (RT-qPCR) was performed for EMT genes, such as *e-cadherin, α-sma*, and *fibronectin* from the cones and peripheral epithelial samples. Results revealed that the mRNA levels of *α-sma* and *fibronectin* were significantly elevated in the extraconal periphery (Fig. 3A). The mRNA levels of *e-cadherin* did not show any change in the cone and extraconal periphery compared to the controls (Fig. 3A). Immunofluorescence staining with ZO-1 revealed weak positivity in the extraconal periphery. Some amount of positivity could be seen in the corneal epithelial cells of the cones (Fig. 3B). Quantification of the number of ZO-1–positive cells did not show any difference in the cones compared to the controls. However, there was a

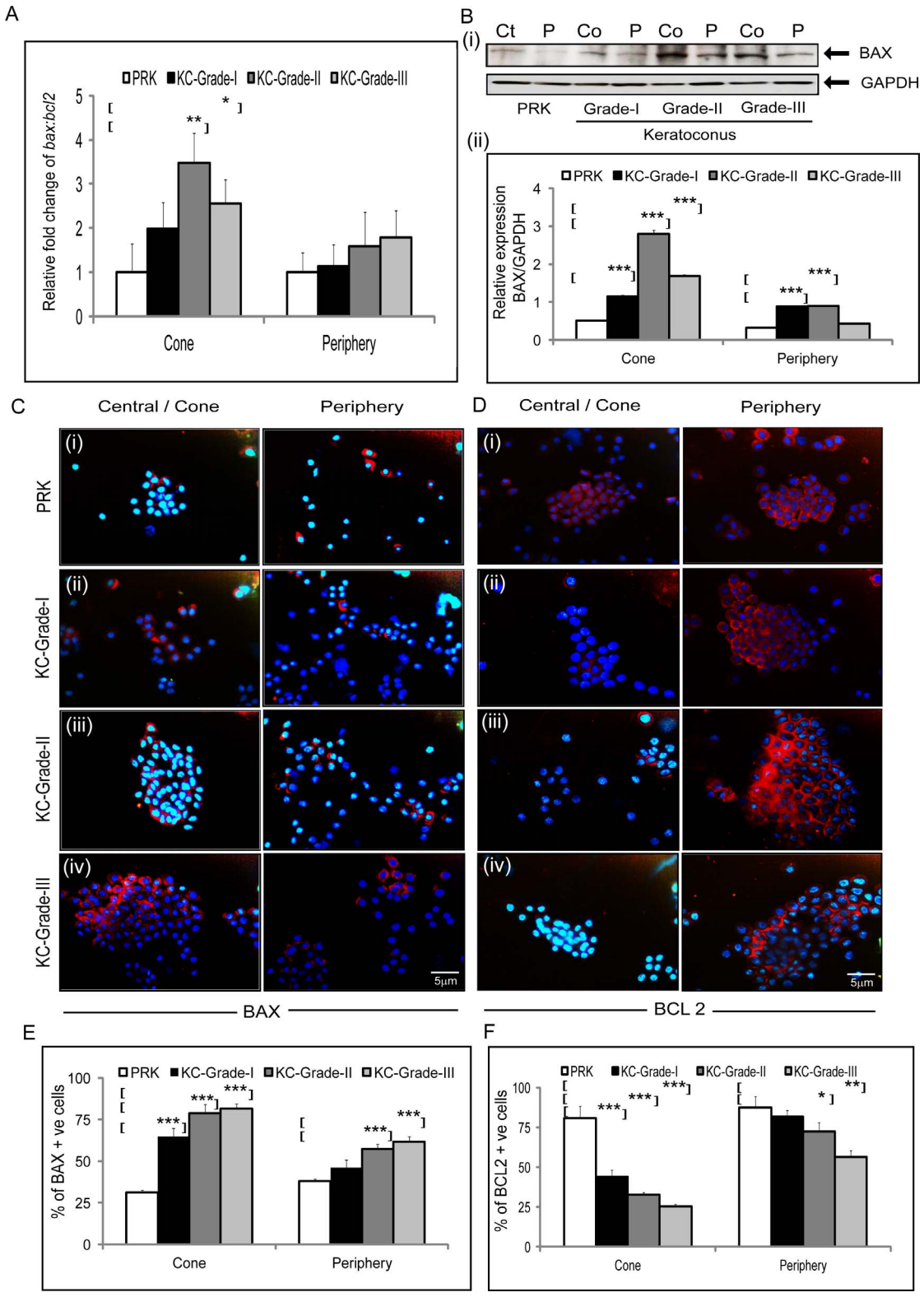

Figure 1. Expression of proapoptotic markers BAX and antiapoptotic markers in corneal epithelial cells of cone and extraconal periphery. Ratio of the RT-qPCR–based expression profile of *bax* and *bcl2* genes in control epithelial cells from PRK (central and peripheral) and different grades of KC (affected cone and unaffected periphery) depicted as relative fold change with respect to control epithelial cells from PRK (A; $n = 4$). Representative Western blot for anti-human BAX antibody in cell lysates obtained from central and →

←
peripheral cornea of control epithelial cells from PRK eyes, and cone and extraconal periphery of grades of KC. Anti-human GAPDH was used as housekeeping protein (Bi). Western blot quantification results (Bii) depicted as relative expression with respect to GAPDH levels ($n = 3$). Representative images of immunofluorescence staining with anti-human BAX (C) and BCL2 (D) antibodies in cytospined corneal epithelial cells collected from central and peripheral cornea of control epithelial cells from PRK eyes, and cone and extraconal periphery of grades of KC ($n = 3$). Secondary antibody anti-rabbit-Cy3 (*Red*) along with counterstain 4′,6-diamidino-2-phenylendole (DAPI; *Blue*) for nuclear staining was used. Percentage of BAX-positive (E) and BCL2-positive (F) cells was counted and depicted. The number of biological samples used for calculating mean ± SD is mentioned as "*n*". Significance denoted as $P \leq 0.05$ (*), $P \leq 0.01$ (**), $P \leq 0.005$ (***). *Scale bar*: 5 μm.

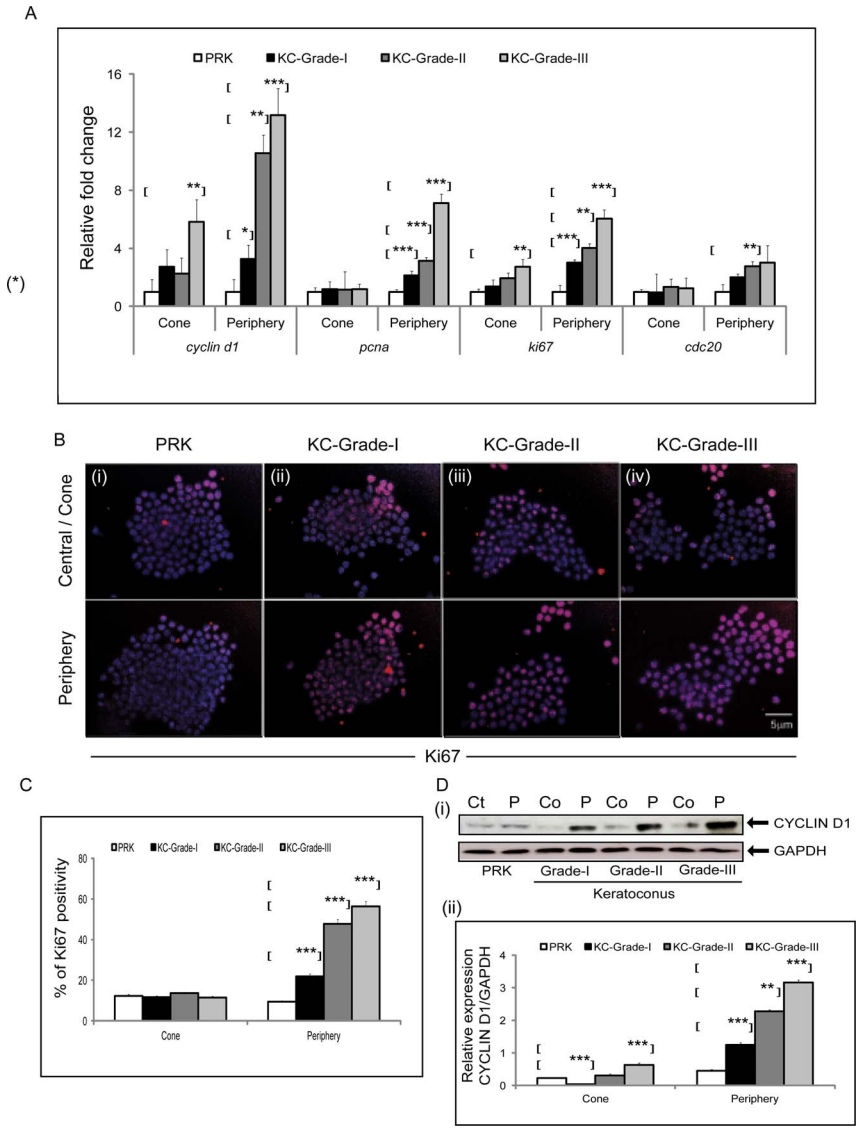

Figure 2. Expression of proliferative markers cyclin D1 and Ki67 in epithelial cells of cone and extraconal periphery. RT-qPCR based relative gene expression of *cyclin c1, ki67, pcna*, and *cdc20* was shown in corneal epithelial cells obtained from central and peripheral cornea of Control epithelial cells from PRK, affected cone and unaffected periphery of KC eyes of different grades (A; $n = 3$). Representative images depicting immunofluorescence staining with anti-human Ki67 on cytospined corneal epithelial cells obtained from PRK and KC eyes of different grades along with counter stain DAPI (*Blue*) for nuclear staining was used. (B) Percentage of Ki-67–positive cells (C) was counted and depicted graphically ($n = 3$). Western blot analysis of cell lysate of KC and Control eyes stained for CYCLIN D1 levels. Anti-human GAPDH was used as housekeeping protein (Di) Densitometric analysis for percentage of CYCLIN D1-positive staining (Dii; $n = 3$). The number of biological samples used for calculating mean ± SD is mentioned as "*n*". Significance denoted as $P \leq 0.01$ (**), $P \leq 0.005$ (***). *Scale bar*: 5 μm.

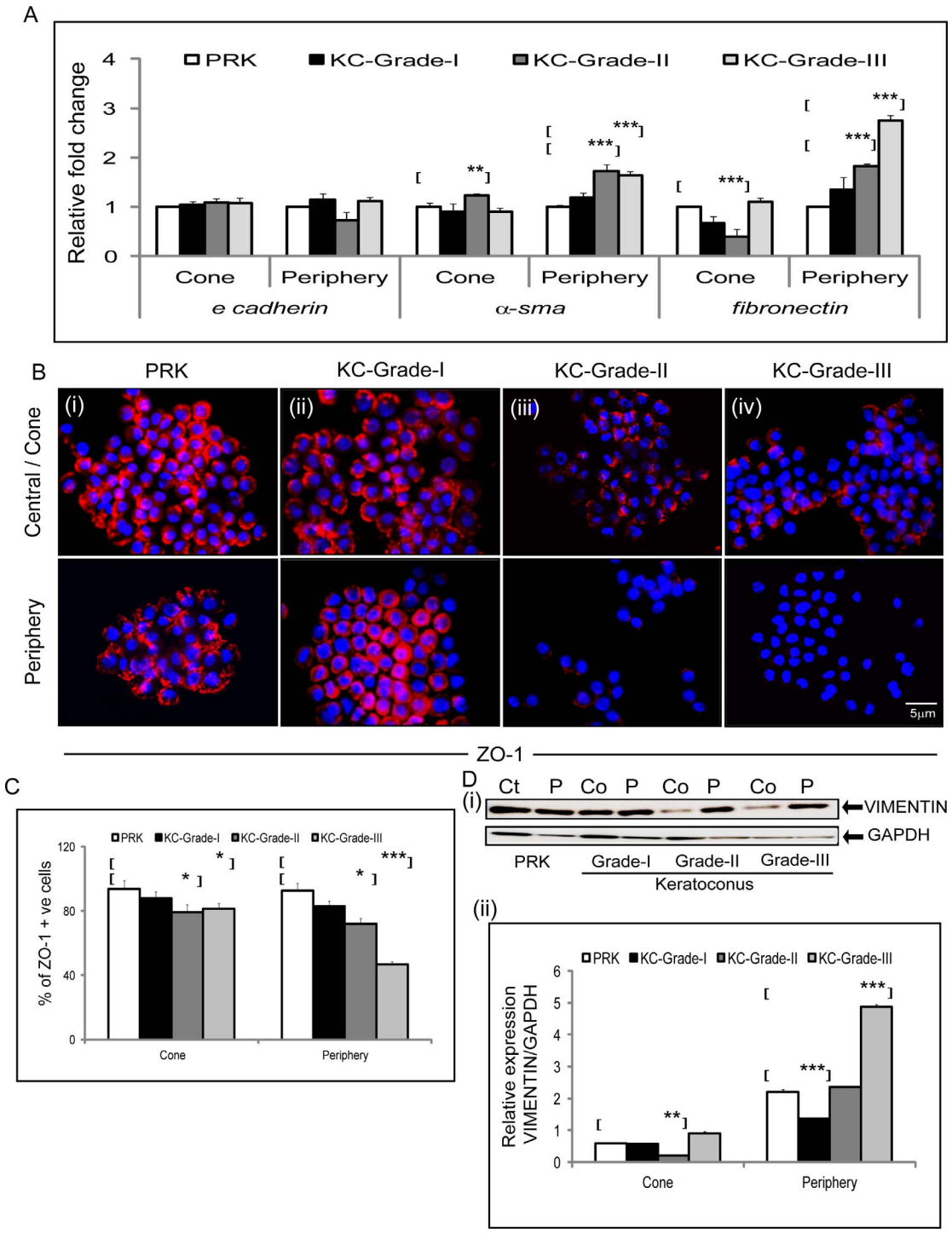

Figure 3. Expression of epithelial-mesenchymal transition markers in corneal epithelial cells of cone and extraconal periphery. RT-qPCR based relative gene expression of *e-cadherin, a-sma*, and *fibronectin* shown in corneal epithelial cells obtained from central and peripheral cornea of PRK, cone, and extraconal periphery of KC eyes of different grades (A; $n = 5$). Representative images depicting immunofluorescence staining with anti-human ZO-1 (B) antibody (Red) on cytospined corneal epithelial cells obtained from PRK and KC eyes of different grades along with counter stain DAPI (*Blue*) for nuclear staining was used. Percentage of ZO-1-positive cells (C) was counted and depicted graphically ($n = 3$). Western blot for anti-human Vimentin antibody in cell lysates obtained from central and peripheral cornea of control epithelial cells from PRK eyes, and cone and extraconal periphery of grades of KC. Anti-human GAPDH was used as housekeeping protein (Di; $n = 3$). Western blot quantification results (Dii) depicted as relative expression with respect to GAPDH levels. The number of biological samples used for calculating mean ± SD is mentioned as "*n*." Significance denoted as $P \leq 0.01$ (**), $P \leq 0.005$ (***). *Scale bar*: 5 μm.

Table 4. Densitometry Values of the Western Blots of Proteins With *P* Values

	PRK		KC Grade I			
Protein	Ce	*P*	C	*P* Value	*P*	*P* Value
BAX	0.5 ± 0.01	0.3 ± 0.004	1.14 ± 0.04	<0.005	0.89 ± 0.01	<0.005
CYCLIN D1	0.22 ± 0.01	0.45 ± 0.04	0.039 ± 0.02	<0.005	1.24 ± 0.08	<0.005
VIMENTIN	0.63 ± 0.05	2.33 ± 0.07	0.61 ± 0.01	NS	1.37 ± 0.1	<0.005
NOTCH 1	0.33 ± 0.02	0.87 ± 0.04	0.38 ± 0.03	NS	1.2 ± 0.02	<0.005
JAGGED 2	0.72 ± 0.03	0.7 ± 0.06	0.17 ± 0.07	<0.005	0.67 ± 0.04	NS

Table 4. Extended

	KC Grade II				KC Grade III			
Protein	C	*P* Value	*P*	*P* Value	C	*P* Value	*P*	*P* Value
BAX	2.8 ± 0.09	<0.005	0.89 ± 0.02	<0.005	1.69 ± 0.03	<0.005	0.43 ± 0.01	NS
CYCLIN D1	0.30 ± 0.05	NS	0.27 ± 0.05	<0.01	0.62 ± 0.06	<0.005	3.15 ± 0.09	<0.005
VIMENTIN	0.21 ± 0.09	<0.01	2.37 ± 0.08	NS	0.98 ± 0.04	NS	4.65 ± 0.07	<0.005
NOTCH 1	1.0 ± 0.01	<0.005	1.23 ± 0.05	<0.005	2.16 ± 0.11	<0.005	1.53 ± 0.08	<0.005
JAGGED 2	0.42 ± 0.03	<0.05	1.45 ± 0.04	<0.005	0.93 ± 0.01	<0.005	2.45 ± 0.03	<0.005

significantly lower number in the extraconal periphery compared to the controls (Fig. 3C). Western blot analysis further corroborated with the cone and periphery results (Fig. 3Di). Densitometric analysis of Western blot showed there was no change in the levels of VIMENTIN in Grade I cone epithelial cells compared to controls, whereas a significant decrease in the levels was noted in the extraconal periphery compared to controls. Grade II results revealed a significant decrease in the levels of VIMENTIN in the cones, but no change in the periphery compared to the controls, whereas in Grade III no change in VIMENTIN levels was noted in the cone, but a significantly higher levels were observed in the periphery compared to the controls. The extraconal periphery showed a trend of increasing levels of VIMENTIN with increasing severity of KC, whereas the cones did not show much change with respect to the controls (Fig. 3Dii).

Corneal Epithelial Differentiation Status in Affected and Unaffected Regions

RT-qPCR for *ck3*/*ck12* gene revealed a decrease in the mRNA levels in epithelial cells from the cone compared to controls, which correlated with the disease severity (Fig. 4A). Additionally, mRNA levels were significantly decreased in cones of KC except in Grade 1 (Fig. 4A). Moreover, there was a significant upregulation in the mRNA levels of *ck3*/*ck12* in the peripheral regions compared to the controls (Fig. 4A). Immunofluorescence staining for CK3/12 revealed a significant decrease in the number of CK3/12 positivity in the cells obtained from the cone with increasing severity of the disease (Fig. 4B), whereas there was a significant increase in the number of CK3/12-positive cells in the KC periphery epithelial cells compared to KC cone epithelial cells as noted in the graphic representation (Fig. 4C). Quantification revealed a significant decrease in the number of CK3/CK12-positive cells in the cones with increasing grades of KC (Fig. 4C). Hence, the results obtained indicate that there is reduced corneal epithelial differentiation in cells located in the cone.

Notch Signaling in KC Cornea

RT-qPCR was performed on the cDNA of corneal epithelial cells collected from the cones and the extraconal periphery. The results showed a significantly elevated mRNA expression of receptor *notch 1* in both regions compared to the controls. The mRNA levels increased with increasing grades of KC. The rest of the notch receptors, such as *notch 2*, *notch 3*, and *notch 4* did not show any significant difference between KC and control (Fig. 5A). Among the ligands, *jagged 2* mRNA showed significantly elevated expressions in both areas compared to the controls. The mRNA levels of the rest of the ligands, such as *delta-like 1, delta-like 3, delta-like 4*, and *jagged 1*, did not show any significant difference between the KC

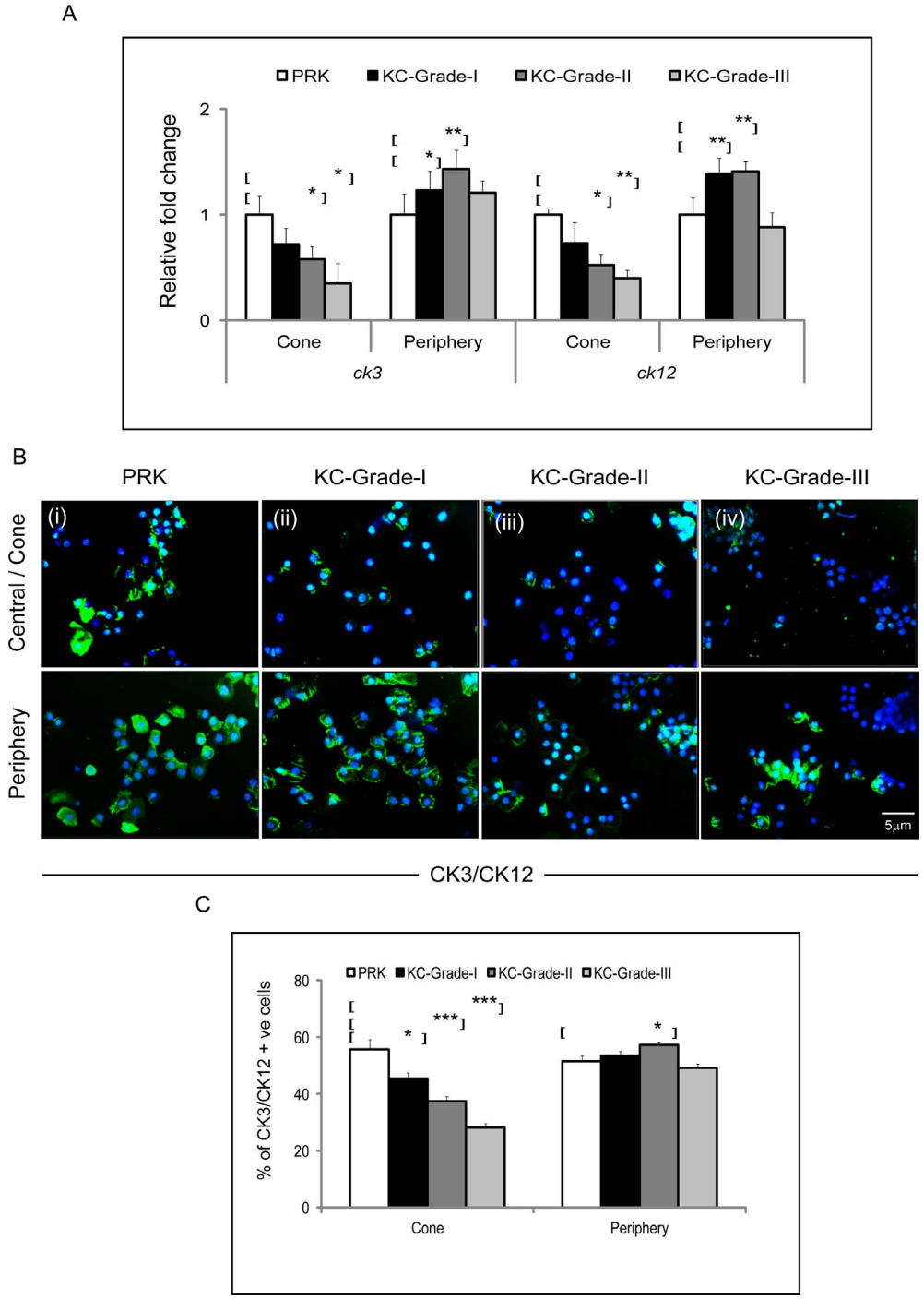

Figure 4. Expression of corneal differentiation marker in corneal epithelial cells of cone and extraconal periphery. RT-qPCR based expression profile of *ck3* and *ck12* genes in control epithelial cells from PRK (central and peripheral) and different grades of KC (cone and extraconal periphery) depicted as relative fold change with respect to control epithelial cells from PRK (A; $n = 3$). Representative images of immunofluorescence staining with antihuman CK3/12 antibody (*Green*) in cytospined corneal epithelial cells collected from central and peripheral cornea of control epithelial cells from PRK eyes, and cone and extraconal periphery of grades of KC along with counter stain DAPI (*Blue*) for nuclear staining was used (B). Percentage of CK3/12-positive cells is counted and depicted (C; $n = 3$). The number of biological samples used for calculating mean ± SD is mentioned as "*n*." Significance denoted as $P \leq 0.05$ (*), $P \leq 0.01$ (**), $P \leq 0.005$ (***). *Scale bar*: 5 μm.

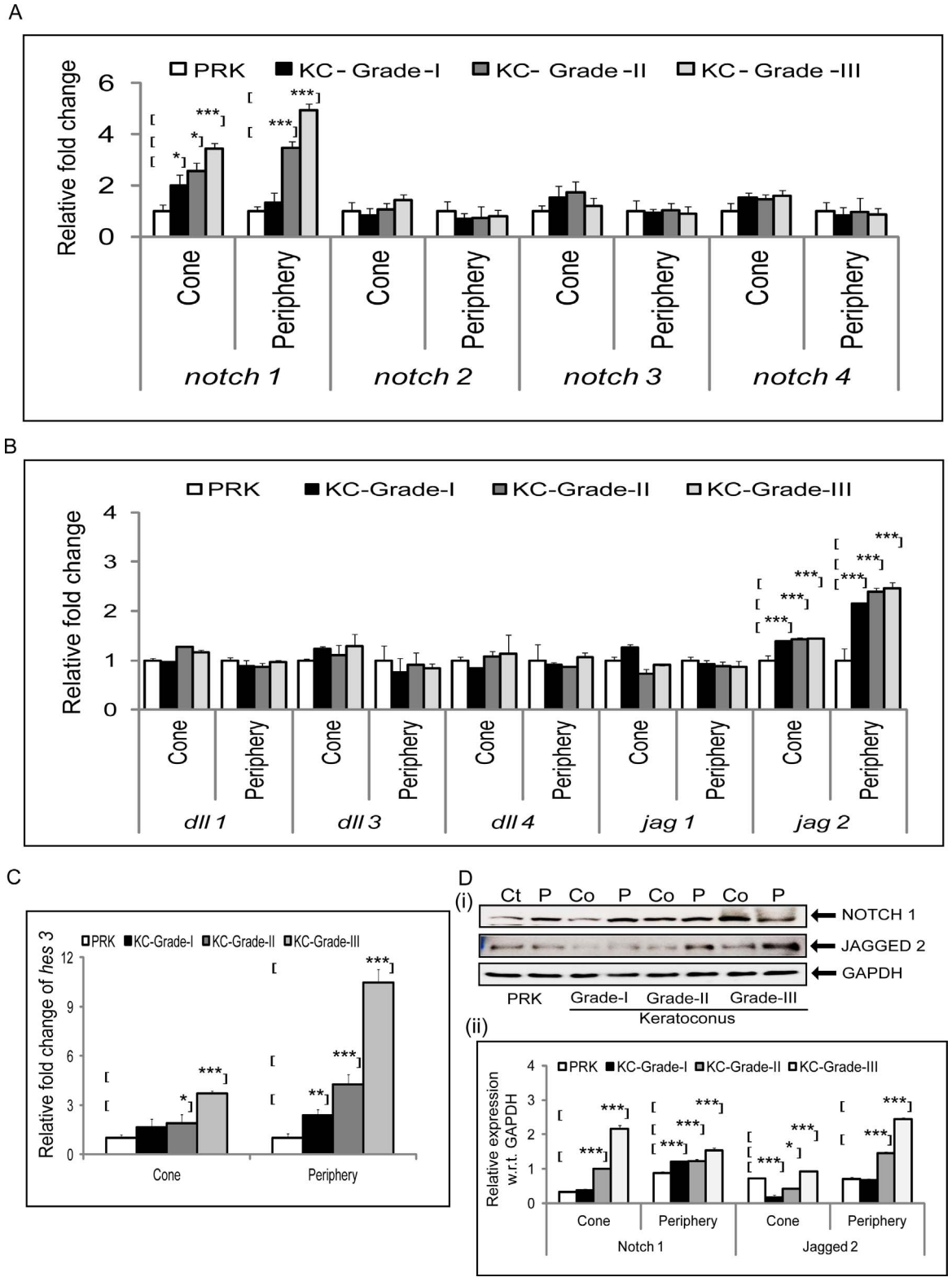

Figure 5. Expression of Notch signaling markers in corneal epithelial cells of cone and extraconal periphery. Expression profile of Notch receptors (A), ligands (B) and downstream target (C) in control epithelial cells from PRK (central and peripheral) and different grades of KC (cone and extraconal periphery) depicted as relative fold change with respect to PRK ($n = 4$). Western blot for anti-human NOTCH 1, anti-human JAGGED 2, antibody in cell lysates obtained from central and peripheral cornea of PRK eyes, and cone and extraconal periphery of →

←
grades of KC. Anti-human GAPDH was used as housekeeping protein (Di; $n = 3$). Western blot quantification results (Dii) depicted as relative expression of NOTCH 1 and JAGGED 2 with respect to GAPDH levels. The number of biological samples used for calculating mean ± SD is mentioned as "*n*." Significance denoted as $P \leq 0.05$ (*), $P \leq 0.01$ (**), $P \leq 0.005$ (***).

cornea and controls (Fig. 5B). Concurrently, mRNA expression of Notch downstream target *hes3* levels was significantly increased in the extraconal periphery epithelial cells and showed an increasing trend with increasing grades of the disease severity. There was an increase in *hes3* mRNA levels in the cones, but this was not significant compared to controls except in Grade III ($P = 0.003$; Fig. 5C). Western blot analysis revealed results in concurrence with the mRNA expression of NOTCH 1 and JAGGED 2 (Fig. 5D[i]). Densitometry analysis of Western blot revealed a significantly higher expression of NOTCH 1 in the cones except in Grade I KC that increased with increasing grades of KC compared to the controls (Fig. 5Dii). The extraconal periphery revealed a significant increase in the level of NOTCH 1 protein expression across all grades of KC epithelium compared to the controls. The expression levels of JAGGED 2 were elevated in the extraconal periphery in Grades II and III compared to the controls (Fig. 5Dii). There was a weakly elevated expression of Jagged 2 in the cones compared to controls.

Discussion

KC is a heterogeneous disease with a plethora of factors affecting its progression. It has a higher prevalence in the Asian population and affects young adults of the productive age group contributing to the increasing financial burden of our society.[23]

The corneal epithelium is the outermost layer of the cornea and harbors three different epithelial cell types, which occupy different strata, superficial cells on the top, followed by wing cells and basal cells at the bottom.[24] The corneal epithelium directly interacts with environment and is exposed to repeated insults warranting a renewal, that replaces the entire cornea in approximately a week.[25,26] Though in KC there is enhanced keratocyte cell death, the site for disease initiation remains elusive, with hypotheses implicating the stromal cells and epithelial cell layer.[27,28] Independent of this, it is well known that a healthy corneal epithelial layer is required for healthy keratocytes in stroma.[11]

The cornea of a KC patient undergoes several alterations leading to the thinning of the cornea. Kim et al.[8] as well as Kaldawy et al.[29] showed, using KC and control corneas, that TUNEL positivity was increased to depths of the corneal epithelial layer in KC patients whereas the same remained superficial in the controls. The basement membrane in KC has an irregular appearance accompanied with breaks.[30] This leads to defective interactions in corneal epithelium and the stroma, which also is associated with altered gene expression.[31,32] Besides apoptosis of keratocytes and structural changes, not much is known about the cellular signaling mechanisms in KC.[29]

Whole proteome analysis, targeted soluble factor analyses and immunohistochemistry of keratoconic corneas and tears have detected proteins related to inflammation, apoptosis, mesenchymal origin, oxidative stress, and endoplasmic reticulum stress.[33–35] In keratoconic corneas, a number of factors, such as CK3, CK12, Gelsolin, S100A4, and Enolase 1, have been altered.[36] Studies by Nielsen et al.,[37] using molecular and biochemical analysis, have shown that five genes, namely *CLC*, *DSG3*, *EMP3*, *S100A2*, and *SLPI,* were differentially expressed in keratoconic corneas compared to controls. They concluded that these genes/proteins may be involved in the disease etiology.[37] Gene expression studies on mRNA from KC and controls also support the protein level data. Since Nielsen et al.[37] analyzed the total corneal epithelium and not the differential one, it would be difficult to interpret the outcome. There is a possibility of cohort bias as it already has been established that KC disease has an ectatic cone and a nonectatic periphery. It has been shown previously that there are different molecular and biochemical fingerprints that distinguish between the affected and unaffected zones.[31]

In a recent study You et al.[33] used RNA-seq analysis to compare corneal epithelial cells from KC and myopia patients. The study reported was based on the Gene Ontology and KEGG pathway analysis that there were differences in cell communication, cell cycle, migration, differentiation, autophagy, and metabolism of arachidonic acid, chondroitin sulfate and unsaturated fatty acids in KC.[33] Kabza et al.,[38] using transcriptomic profiling analysis on 25 keratoconic and 25 nonkeratoconic corneal tissues, identified the downregulation of transforming growth factor β (TGF-β), Hippo, and Wnt pathways in KC

Table 5. Quantitative Values of Immunofluorescence of Proteins With *P* Values

	PRK		KC Grade I			
Protein	Ce	*P*	C	*P* Value	*P*	*P* Value
BAX	31.3 ± 0.01	38.1 ± 1.3	64.8 ± 5.1	<0.005	46 ± 4.7	NS
BCl2	80.7 ± 7.6	87.4 ± 7.1	44 ± 4.2	<0.005	81.6 ± 4.2	NS
Ki67	12.2 ± 0.88	9.4 ± 0.63	11.72 ± 0.52	NS	21.88 ± 1.39	<0.005
ZO-1	93.7 ± 5.2	92.5 ± 4.8	87.8 ± 4.1	NS	82.8 ± 3.2	NS
CK3/12	55.8 ± 3.32	51.6 ± 1.9	45.4 ± 2.1	<0.05	53.6 ± 1.4	NS

Table 5. Extended

	KC Grade II				KC Grade III			
Protein	C	*P* Value	*P*	*P* Value	C	*P* Value	*P*	*P* Value
BAX	78.9 ± 5.3	<0.005	57.2 ± 3.1	<0.005	81.5 ± 3.1	<0.005	61.7 ± 3.3	<0.005
BCl2	32.7 ± 1.5	<0.005	72.4 ± 5.5	<0.01	25.3 ± 1.4	<0.005	56.4 ± 3.9	<0.05
Ki67	13.67 ± 0.55	NS	47.69 ± 2.43	<0.005	11.47 ± 0.77	NS	56.25 ± 2.74	<0.005
ZO-1	79.1 ± 4.8	<0.05	72.1 ± 3.2	<0.05	81.4 ± 3.2	<0.05	46.6 ± 1.7	<0.005
CK3/12	37.5 ± 1.7	<0.005	57.3 ± 1.1	<0.05	28.2 ± 1.4	<0.005	49.1 ± 1.6	NS

corneas. Wnt signaling is downregulated with a simultaneous increase in SFRP1 levels in KC corneas, though there is a decrease in the SFRP1 levels in tears of KC patients.[39–41] In genome wide association studies using KC samples, it was found that WNT10A and WNT 7B are important for maintaining the corneal thickness and an exonic variant of WNT10A increases the risk of KC 2-fold.[42,43]

One major limitation of these studies is that they have either used the total cornea or total corneal epithelium, though it is well known that the epithelial cells in the cone and extraconal periphery are morphologically different in KC patients with a distinct molecular expression profile. Therefore, using the entire cornea for the studies may lead to masking of the expression levels from the ectatic zones of the cornea. In our study, we found a higher level of apoptosis in the epithelium of the cone of keratoconic corneas compared to controls. Moreover, apoptosis levels of affected cones increased with increasing grades of KC. These results suggested that the increased apoptosis in KC corneas with the expression of BAX is predominant in the cone areas and correlates with increasing disease severity (Fig. 1). To our knowledge, this is the first report showing elevated apoptosis in corneal epithelial cells in the cone. Kaldawy et al.[8] reported TUNEL staining and single-strand DNA analysis positivity in KC cornea to detect elevated levels of apoptosis. Though increased corneal epithelial cell death in KC eyes has been speculated, it has so far not been demonstrated. This process might cause stromal collagen instability leading to an inflammatory response and disease initiation. The dying cells in the affected cone could cause stress on corneal epithelial cells, possibly making them more susceptible to any external injury. Murine models also have shown that injury to epithelial cells can lead to keratocyte death by IL-1 and induction of Fas ligand.[9,10] Our results revealed higher positivity of proliferative markers (*cyclin D1* and *Ki67*) in the extraconal periphery compared to controls (Fig. 2). It can be very well envisaged that the dying epithelial cells in the cone might trigger a proliferative signal to the adjacent extraconal periphery in an attempt to compensate for the damaged layer. Moreover, we saw a higher positivity of proliferative markers with increasing severity of the disease. Mace et al.,[44] by performing genome wide transcriptional analysis on corneas removed from 10 KC and an equal number of controls concluded antiproliferative and hyperapoptotic genes to be responsible for pathogenesis of KC. It is possible that their findings are different from ours as they used the total cornea and not the affected epithelium selectively.[44] Moreover, though it is of vital importance to segregate the samples for analysis based on their clinical severity, Mace et al.[44] have not provided any information on the grading of

their samples. Studying the total cornea and non-classification of the KC samples could be the reason for the difference in our results compared to those of Mace et al.[44] Besides proliferation, the two additional aspects needed for repopulating the cornea are differentiation and migration. The results showed increase in levels of Vimentin expression and contrarily significantly lower levels of ZO-1 positivity in the extraconal periphery of KC corneas compared to controls, suggesting a probability of higher levels of EMT transition (Fig. 3). Vimentin acts as a signal connector by regulating the structure and function of focal adhesion during EMT.[45] It has been shown that there is upregulation of secreted frizzled related protein (SFRP) a known antagonist of WNT pathway in KC corneal epithelium.[46] WNT pathway has a vital role in modulating EMT. In ovarian cancer cells and retinal pigment epithelial cells, it has been shown that SFRP supplementation or blockage of the Wnt pathway reduced EMT in the cells.[47,48] Connective tissue growth factor (CTGF) is a known inducer of EMT.[49] However, it has been shown that CTGF expression is significantly lower in cornea of KC compared to control.[38] Collagen I, the predominant type of collagen in cornea, is regulated by EMT.[24] Based on our results, it can be postulated that in epithelial cells of the cone, lower collagen levels resulted in lower EMT induction. This implies that there might be higher levels of collagen and CTGF with conversely lower levels of SFRP in the periphery compared to the cone in KC eyes, suggesting higher EMT induction. Though the EMT induction is higher in the periphery, there could be a lag in mesenchymal-epithelial transition (MET) in the cone, thereby not restoring the cells at the corneal cone. Ovo-like zinc finger (Ovol) family of zinc-finger transcription factor proteins are known to mediate MET.[50] In skin-keratinocytes it has been shown that Ovol2 suppresses Notch signaling.[51] Ovol2, one of the family members, is crucial in maintaining the transcriptional program of corneal epithelial cells by repressing mesenchymal genes and EMT.[52] Hence, it could be plausible that there might be lower MET levels in the cone of KC along with lower corneal epithelial cells. There is a significantly lower level of CK3/CK12 positivity in the affected cone of keratoconic corneas, implying lower numbers of matured corneal epithelial cells (Fig. 4). Our results highlighted the cellular changes that occur not only in the cone, but also on its consequences in the extraconal periphery. These results also show for the first time to our knowledge that the cellular changes in the extraconal periphery are suggestive of an attempt by the cornea to compensate for the cone by mobilizing cells from the extraconal periphery. A similar phenomenon is observed in gastrointestinal tract upon injury. In an attempt for early epithelial restitution, healthy cells from areas adjacent to the injury (caused by inflammatory bowel disease) proliferate, migrate, and differentiate apart from repolarizing.[53] Any defect in the mucosal restitution results in disruption of the epithelial integrity and barrier dysfunction leading to pathologic consequences.[54]

Corneal epithelial cells residing in the cone showed higher cellular apoptosis (*bax* / *bcl2* marker ratio). There was an increased proliferation as shown by *ki67* and *cyclin D1* levels at the peripheral cornea. There was a higher expression of EMT markers in the periphery compared to controls. Expression of CK3/CK12, which is a definitive marker for corneal epithelial cells, was reduced in the cone (Fig. 4). This suggested that crosslinking procedures might be more effective if they are focused on the affected area alone. Schematic representation of summary of the status of various marker is depicted in Figure 6.

We further analyzed Notch signaling, which has been implicated in the proliferation and differentiation of corneal/limbal epithelial cells.[14] In a recent study, You et al.[33] showed, using total corneal epithelial cells of KC and myopia patients by RNA-Seq, that there is a downregulation of Notch signaling in KC compared to controls. Though they showed reduction in RNA and protein expression levels of Notch1, they could not show any significant difference in levels of Notch intracellular domain (NICD) between corneal epithelial cells of KC and myopia patients.[33] In our study, in addition to showing the expression of Notch receptors and ligands, we have provided the mRNA levels of Hes3, a basic-helix-loop-helix downstream target of Notch signaling. This suggested that elevated expression of Notch signaling components is associated with elevated activity of Notch signaling. The difference in the results of You et al.[33] with our data could be attributed to aspects of clinical segregation of the samples used in the respective studies. We used cone and periphery-specific epithelium separately to avoid any masking of the protein or mRNA expression of the genes of interest from the diseased area, where as You et al.[33] used total corneal epithelium for the RNA-Seq analysis. Additionally we classified our sample cohort based on severity of the disease to

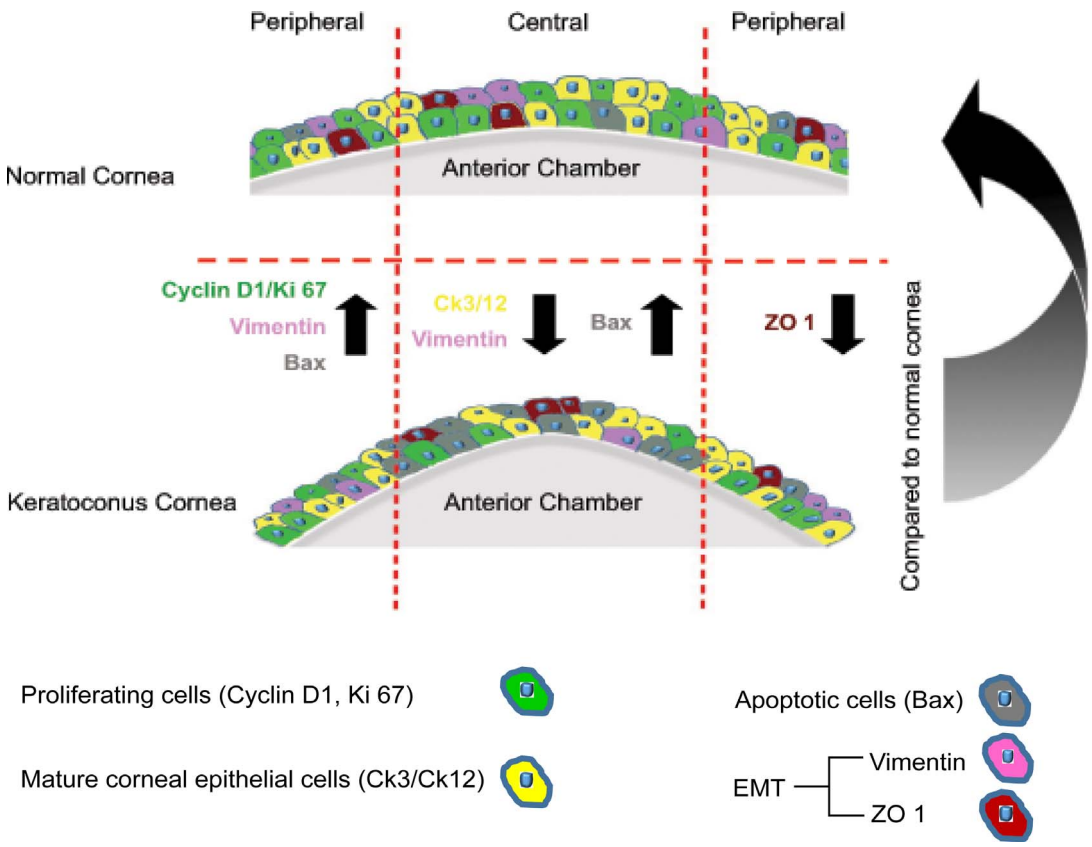

Figure 6. Schematic representation of keratoconic and nonkeratoconic cornea. Schematic representation summarizing the expression of markers in cone and the extraconal periphery of keratoconic cornea. Increased expression of proapoptotic marker (BAX), decreased expression of proliferative markers (Cyclin D1, Ki67), corneal maturation marker (CK3/CK12), and EMT markers was seen in the affected cone. In the unaffected periphery there was increased expression of proliferative markers (Cyclin D1, Ki67), EMT markers and corneal maturation marker (CK3/CK12).

better investigate the correlation of altered gene expression with disease stage.

Compared to the cones, the cells in the extraconal periphery had higher levels of Notch activation and EMT induction. Expression of notch 1 receptor sequentially increased in the affected corneal epithelial cells with increasing disease severity. Notch signaling is known to regulate cellular proliferation by activating Cyclin D1, a G0/G1 cell cycle regulator.[25] The findings suggested that there is a possibility that limbal epithelial cells in KC eyes might be highly active to repopulate the dead corneal epithelial cells on the corneal surface. In KC eyes, an already compromised limbal epithelial cell milieu due to chronic allergy (vernal keratoconujunctivitis [VKC]), precludes a higher possibility of failure with the CXL procedure. KC eyes associated with VKC progress much faster than those without. It also has been shown in children that the presence of VKC results in failure of CXL.[26] This suggests that the failure of the treatment in such a disease phenotype might have a cellular predisposition implicating that compromised limbal cells may not be able to restore the corneal surface after CXL.

The limitations of our study included the small sample size as well as the limited number of markers tested. However, in the absence of an appropriate animal model of KC, studies on patient samples remain the only recourse having the inherent limitation of being small in quantity. Nonetheless, the study results open up new areas in KC biology with implications for future treatment.

Customized crosslinking is a technique of providing eccentric localized UV irradiation to the cone. It uses zones that are concentric over the maximum elevated point on posterior elevation maps.[55] This cone-specific and graded decrease in the amount of UV-A irradiation provided to the periphery has been shown to be as effective as traditional crosslinking without the risk of exposure of irradiation to the

limbal cells. Given the observations from this study, a cone-centered crosslinking could be a better practice in the long term. Ex vivo studies comparing limbal stem cell health after crosslinking using traditional versus customized techniques is the need of the hour.

Acknowledgments

The authors thank Krishna Bhujang Shetty and Pindipanahalli Narendra, Narayana Nethralaya, Bangalore, India for their administrative support and for providing the necessary logistics for this study.

Supported by Narayana Nethralaya Foundation, Bangalore, India and Department of Science and Technology, Government of India (SR/SO/HS/0228/2012) and Science and Enginnering Research Board, Government of India (EMR/2016/003624).

Disclosure: **R. Shetty**, None; **K.P. Vunnava**, None; **K. Dhamodaran**, None; **H. Matalia**, None; **S. Murali**, None; **C. Jayadev**, None; **P. Murugeswari**, None; **A. Ghosh**, None; **D. Das**, None

References

1. Jeyabalan N, Shetty R, Ghosh A, Anandula VR, Ghosh AS, Kumaramanickavel G. Genetic and genomic perspective to understand the molecular pathogenesis of keratoconus. *Indian J Ophthalmol*. 2013;61:384–388.
2. Ghosh A, Zhou L, Ghosh A, Shetty R, Beuerman R. Proteomic and gene expression patterns of keratoconus. *Indian J Ophthalmol*. 2013;61:389–391.
3. Karolak JA, Gajecka M. Genomic strategies to understand causes of keratoconus. *Mol Genet Genomics*. 2017;292:251–269.
4. Shetty R, Ghosh A, Lim RR, et al. Elevated expression of matrix metalloproteinase-9 and inflammatory cytokines in keratoconus patients is inhibited by cyclosporine A. *Invest Ophthalmol Vis Sci*. 2015;56:738–750.
5. Shetty R, Sathyanarayanamoorthy A, Ramachandra RA, et al. Attenuation of lysyl oxidase and collagen gene expression in keratoconus patient corneal epithelium corresponds to disease severity. *Mol Vi.s* 2015;21:12–25.
6. Shetty R. Keratoconus and corneal collagen cross-linking. *Indian J Ophthalmol*. 2013;61:380.
7. Somodi S, Hahnel C, Slowik C, Richter A, Weiss DG, Guthoff R. Confocal in vivo microscopy and confocal laser-scanning fluorescence microscopy in keratoconus. *German J Ophthalmol*. 1996;5:518–525.
8. Kaldawy RM, Wagner J, Ching S, Seigel GM. Evidence of apoptotic cell death in keratoconus. *Cornea*. 2002;21:206–209.
9. Mohan RR, Liang Q, Kim WJ, Helena MC, Baerveldt F, Wilson SE. Apoptosis in the cornea: further characterization of Fas/Fas ligand system. *Exp Eye Res*. 1997;65:575–589.
10. Wilson SE, He YG, Weng J, et al. Epithelial injury induces keratocyte apoptosis: hypothesized role for the interleukin-1 system in the modulation of corneal tissue organization and wound healing. *Exp Eye Res*. 1996;62:325–327.
11. Sherwin T, Brookes NH. Morphological changes in keratoconus: pathology or pathogenesis. *Clin Exp Ophthalmol*. 2004;32:211–217.
12. Sharif R, Fowler B, Karamichos D. Collagen cross-linking impact on keratoconus extracellular matrix. *PloS One*. 2018;13:e0200704.
13. Matalia H, Shetty R, Dhamodaran K, Subramani M, Arokiaraj V, Das D. Potential apoptotic effect of ultraviolet-A irradiation during cross-linking: a study on ex vivo cultivated limbal epithelial cells. *Br J Ophthalmol*. 2012;96:1339–1345.
14. Shetty R, Matalia H, Nuijts R, et al. Safety profile of accelerated corneal cross-linking versus conventional cross-linking: a comparative study on ex vivo-cultured limbal epithelial cells. *Br J Ophthalmol*. 2015;99:272–280.
15. Vimalin J, Gupta N, Jambulingam M, Padmanabhan P, Madhavan HN. The effect of riboflavin-UV-A treatment on corneal limbal epithelial cells–a study on human cadaver eyes. *Cornea*. 2012;31:1052–1059.
16. Al-Qarni A, AlHarbi M. Herpetic keratitis after corneal collagen cross-linking with riboflavin and ultraviolet-A for keratoconus. *Middle East AJ Ophthalmol*. 2015;22:389–392.
17. Hollhumer R, Watson S, Beckingsale P. Persistent epithelial defects and corneal opacity after collagen cross-linking with substitution of dextran (T-500) with dextran sulfate in compounded topical riboflavin. *Cornea*. 2017;36:382–385.
18. Vinciguerra R, Romano V, Arbabi EM, et al. In vivo early corneal biomechanical changes after corneal cross-linking in patients with progressive keratoconus. *J Refract Surg*. 2017;33:840–846.

19. Wojcik KA, Blasiak J, Szaflik J, Szaflik JP. Role of biochemical factors in the pathogenesis of keratoconus. *Acta Biochim Pol*. 2014;61:55–62.
20. Roy AS, Shetty R, Kummelil MK. Keratoconus: a biomechanical perspective on loss of corneal stiffness. *Indian J Ophthalmol*. 2013;61:392–393.
21. Shetty R, Rajiv Kumar N, Pahuja N, et al. Outcomes of corneal cross-linking correlate with cone-specific lysyl oxidase expression in patients with keratoconus. *Cornea*. 2018;37:369–374.
22. Dhamodaran K, Subramani M, Jeyabalan N, et al. Characterization of ex vivo cultured limbal, conjunctival, and oral mucosal cells: A comparative study with implications in transplantation medicine. *Mol Vis*. 2015;21:828–845.
23. Rabinowitz YS. Keratoconus. *Surv Ophthalmol*. 1998;42:297–319.
24. Torricelli AA, Singh V, Santhiago MR, Wilson SE. The corneal epithelial basement membrane: structure, function, and disease. *Invest Ophthalmol Vis Sci*. 2013;54:6390–6400.
25. Yazdanpanah G, Jabbehdari S, Djalilian AR. Limbal and corneal epithelial homeostasis. *Curr Opin Ophthalmol*. 2017;28:348–354.
26. Yoon JJ, Ismail S, Sherwin T. Limbal stem cells: Central concepts of corneal epithelial homeostasis. *World J Stem Cells*. 2014;6:391–403.
27. Song P, Wang S, Zhang P, et al. The superficial stromal scar formation mechanism in keratoconus: a study using laser scanning in vivo confocal microscopy. *BioMed Res Int*. 2016;2016:7092938.
28. Tsubota K, Mashima Y, Murata H, Sato N, Ogata T. Corneal epithelium in keratoconus. *Cornea* 1995;14:77–83.
29. Kim WJ, Rabinowitz YS, Meisler DM, Wilson SE. Keratocyte apoptosis associated with keratoconus. *Exp Eye Res*. 1999;69:475–481.
30. Teng CC. Electron microscope study of the pathology of keratoconus: I. *Am J Ophthalmol*. 1963;55:18–47.
31. Pahuja N, Kumar NR, Shroff R, et al. Differential molecular expression of extracellular matrix and inflammatory genes at the corneal cone apex drives focal weakening in keratoconus. *Invest Ophthalmol Vis Sci*. 2016;57:5372–5382.
32. Cheng EL, Maruyama I, SundarRaj N, Sugar J, Feder RS, Yue BY. Expression of type XII collagen and hemidesmosome-associated proteins in keratoconus corneas. *Curr Eye Res*. 2001;22:333–340.
33. You J, Corley SM, Wen L, et al. RNA-Seq analysis and comparison of corneal epithelium in keratoconus and myopia patients. *Sci Rep*. 2018;8:389.
34. Nishtala K, Pahuja N, Shetty R, Nuijts RM, Ghosh A. Tear biomarkers for keratoconus. *Eye Vis (Lond)*. 2016;3:19.
35. Chaerkady R, Shao H, Scott SG, Pandey A, Jun AS, Chakravarti S. The keratoconus corneal proteome: loss of epithelial integrity and stromal degeneration. *J Proteomics*. 2013;87:122–131.
36. Nielsen K, Vorum H, Fagerholm P, et al. Proteome profiling of corneal epithelium and identification of marker proteins for keratoconus, a pilot study. *Exp Eye Res*. 2006;82:201–209.
37. Nielsen K, Heegaard S, Vorum H, Birkenkamp-Demtroder K, Ehlers N, Orntoft TF. Altered expression of CLC, DSG3, EMP3, S100A2, and SLPI in corneal epithelium from keratoconus patients. *Cornea*. 2005;24:661–668.
38. Kabza M, Karolak JA, Rydzanicz M, et al. Collagen synthesis disruption and downregulation of core elements of TGF-beta, Hippo, and Wnt pathways in keratoconus corneas. *Eur J Hum Genet*. 2017;25:582–590.
39. Khaled ML, Bykhovskaya Y, Yablonski SER, et al. Differential expression of coding and long noncoding RNAs in keratoconus-affected corneas. *Invest Ophthalmol Vis Sci*. 2018;59:2717–2728.
40. Sutton G, Madigan M, Roufas A, McAvoy J. Secreted frizzled-related protein 1 (SFRP1) is highly upregulated in keratoconus epithelium: a novel finding highlighting a new potential focus for keratoconus research and treatment. *Clin Exp Ophthalmol*. 2010;38:43–48.
41. You J, Hodge C, Wen L, McAvoy JW, Madigan MC, Sutton G. Tear levels of SFRP1 are significantly reduced in keratoconus patients. *Mol Vis*. 2013;19:509–xxx.
42. Cuellar-Partida G, Springelkamp H, Lucas SE, et al. WNT10A exonic variant increases the risk of keratoconus by decreasing corneal thickness. *Hum Mol Genet*. 2015;24:5060–5068.
43. Gao X, Nannini DR, Corrao K, et al. Genome-wide association study identifies WNT7B as a novel locus for central corneal thickness in Latinos. *Hum Mol Genet*. 2016;25:5035–5045.
44. Mace M, Galiacy SD, Erraud A, et al. Comparative transcriptome and network biology analyses demonstrate antiproliferative and hyperapoptotic phenotypes in human keratoconus corneas. *Invest Ophthalmol Vis Sci*. 2011;52:6181–6191.
45. Mendez MG, Kojima S, Goldman RD. Vimentin induces changes in cell shape, motility, and adhesion during the epithelial to mesenchymal transition. *FASEB J*. 2010;24:1838–1851.

46. You J, Wen L, Roufas A, Madigan MC, Sutton G. Expression of SFRP family proteins in human keratoconus corneas. *PloS One*. 2013;8:e66770.
47. Ford CE, Jary E, Ma SS, Nixdorf S, Heinzelmann-Schwarz VA, Ward RL. The Wnt gatekeeper SFRP4 modulates EMT, cell migration and downstream Wnt signalling in serous ovarian cancer cells. *PloS One*. 2013;8:e54362.
48. Chen HC, Zhu YT, Chen SY, Tseng SC. Wnt signaling induces epithelial-mesenchymal transition with proliferation in ARPE-19 cells upon loss of contact inhibition. *Lab Invest*. 2012;92: 676–687.
49. Sonnylal S, Xu S, Jones H, et al. Connective tissue growth factor causes EMT-like cell fate changes in vivo and in vitro. *J Cell Sci*. 2013;126: 2164–2175.
50. Liu J, Wu Q, Wang Y, et al. Ovol2 induces mesenchymal-epithelial transition via targeting ZEB1 in osteosarcoma. *OncoTargets Ther*. 2018; 11:2963–2973.
51. Wells J, Lee B, Cai AQ, et al. Ovol2 suppresses cell cycling and terminal differentiation of keratinocytes by directly repressing c-Myc and Notch1. *J Biol Chem*. 2009;284:29125–29135.
52. Kitazawa K, Hikichi T, Nakamura T, et al. OVOL2 Maintains the transcriptional program of human corneal epithelium by suppressing epithelial-to-mesenchymal transition. *Cell Rep*. 2016;15: 1359–1368.
53. Lacy ER. Epithelial restitution in the gastrointestinal tract. *J Clin Gastroent*. 1988;10(suppl 1): S72–77.
54. Sturm A, Dignass AU. Epithelial restitution and wound healing in inflammatory bowel disease. *World J Gastroent*. 2008;14:348–353.
55. Sinha Roy A, Dupps WJ Jr. Patient-specific computational modeling of keratoconus progression and differential responses to collagen cross-linking. *Invest Ophthalmol Vis Sci*. 2011;52:9174–9187.